JOURNAL OF Applied Polymer SCIENCE

Dielectric and Thermal Studies of the Segmental Dynamics of Poly(methyl methacrylate)/Silica Nanocomposites Prepared by the Sol-Gel Method

Konstantinos Kyriakos,[1] Konstantinos N. Raftopoulos,[1] Polycarpos Pissis,[1] Apostolos Kyritsis,[1] Franziskus Näther,[2] Liane Häußler,[2] Dieter Fischer,[2] Anastasia Vyalikh,[2] Ulrich Scheler,[2] Uta Reuter,[2] Doris Pospiech[2]

[1]Department of Physics, National Technical University of Athens, Iroon Polytechneiou 9, 15780 Athens, Greece
[2]Leibniz-Institut für Polymerforschung Dresden e.V., Hohe Str. 6, 01069 Dresden, Germany
*Present address: Fachgebiet Physik weicher Materie, Physik Department, Technische Universität München, James-Franck-Strasse 1, 85747 Garching, Germany.
Correspondence to: K. Kyriakos (konstantinos.kyriakos@tum.de)

ABSTRACT: Poly(methyl methacrylate)/silica (PMMA/SiO_x) nanocomposites were synthesized via sol–gel method and studied by various techniques. The dispersion of the silica particles (10–100 nm) in the matrix was probed by transmission electron microscopy (TEM), while solid-state NMR and Raman spectroscopy detected the formation of an inorganic network with high degree of cross-linking. To elucidate the impact of the filler on the molecular dynamics of the PMMA, different methods were used; namely differential scanning calorimetry, thermally stimulated depolarization current and broadband dielectric relaxation spectroscopy. All three methods observed a significant impact of the nanoparticles on the segmental dynamics of the matrix, which was expressed as an increase of the glass transition temperature (T_g) in terms of calorimetry and as a shift of the α (segmental) relaxation to lower frequencies in terms of dielectric spectroscopy. © 2012 Wiley Periodicals, Inc. J. Appl. Polym. Sci. 128: 3771–3781, 2013

KEYWORDS: glass transition; composites; nanoparticles; nanowires and nanocrystals; differential scanning calorimetry

Received 11 July 2012; accepted 19 September 2012; published online 10 October 2012
DOI: 10.1002/app.38599

INTRODUCTION

In the recent years, hybrid materials consisting of an organic matrix with embedded inorganic nanofillers have attracted major attention. The synergy on a molecular level between the physical and chemical properties of each phase is expected to influence favorably the macroscopic properties (enhanced mechanical strength, thermal stability, higher chemical resistance, high conductivity, etc.). Therefore, a lot of research efforts have been made to develop new nanocomposite materials, and new characterization methods were applied to understand the impact of nanofiller distribution and phase adhesion on the resulting properties better.[1–3]

One of the main contributions of nanoscaled fillers is that very low content is sufficient to achieve the desirable properties. The reason for the significant improvement of the macroscopic properties at very low-filler contents is the very high surface to volume ratio of nanoparticles. Thus, in some systems, even at contents as low as 1–2 vol %, a very strong effect of the filler on the matrix properties is observed.[4] It is commonly accepted that the modification of properties in polymer nanocomposites is related to the modified polymer dynamics in the interfacial layer between polymer and nanoparticles.[5,6] The presence of various nanofillers, such as silica, nanoclays, titania, and metal nanoparticles, leads, in most of the cases, to the restriction of polymer mobility and ability to thermal transitions.[7–10] In some exceptions, the impact of the filler is completely differing[11–13] mainly due to different type of polymer matrix and filler and/or due to different preparation/processing conditions. Considering all the different results obtained for different nanocomposite systems, it has to be noticed that there is still a high number of open questions to be solved.

Poly(methyl methacrylate) (PMMA) is one of the most studied polymers in the literature due to the very wide range of its applications, for instance, for optical lenses, transparent packaging material, shower constructions, and so on.[14,15] Consequently, nanocomposite materials with PMMA matrix and various fillers have also attracted a lot of attention during recent years. Several different systems of PMMA/(nano)filler have been

studied with different filler selections (e.g., nanoclay,[16] Ag,[17] and SiO_2[18]). Each filler selection aims to improve a specific characteristic of the PMMA matrix, like optical transparency, barrier properties, and thermal stability, to name just a few. PMMA/silica nanocomposites have been the subject of thorough studies mainly due to the intimate contact between the polymer chain and the hydroxyl groups always existing at the silica surface. The H-bridges formed give rise to a strong interaction between PMMA matrix and silica nanoparticles, thus improving phase adhesion and interfacial strength between polymer matrix and nanoparticles, finally improving the impact strengths of the hybrid. Several routes have been explored to introduce silica particles in a polymer matrix in general and PMMA in particular. A brief survey has been given by Wen.[18] Despite the thorough study of this kind of systems, still the results are contradictory, especially with respect to the influence of the filler on the PMMA dynamics and flexibility. Some studies detected a significant effect of the silica on the segmental dynamics of the PMMA either by increasing the glass transition temperature T_g,[19] due to the restriction of chain mobility caused by the interactions between nanoparticles and matrix, or, in contrast, by decreasing it.[20] The latter result was discussed in terms of the increase of free volume caused by the presence of the particles in the matrix. Finally, other studies reported no significant change,[21] as a possible result of superimposition of the aforementioned factors. Beside these observations, a strong interest has arisen recently to understand the behavior of the secondary relaxation β of PMMA in PMMA/silica nanocomposites and to explore the possibility of using β as a probe of the evolution of physical aging. Again, the results reported by various groups are contradictory, because some detect a strong effect of the silica on the β relaxation,[22] while others observed no significant change.[23]

It becomes clear from the brief survey mentioned earlier that, despite the number of published works about the effect of silica on PMMA, still the picture is far from being complete. In the present work, a study of nanocomposites consisting of a PMMA matrix with silica particles as nanofillers produced in the polymer solution *in situ* by sol–gel method is presented. Different characterization methods were applied in order to enlighten the interactions between the polymer chains and the particles and also to determine how these interactions affect the molecular mobility and thermal behavior of the matrix. Thus, differential scanning calorimetry (DSC), thermally stimulated depolarization currents (TSDC), and dielectric relaxation spectroscopy (DRS) were applied as main methods for that study. The internal structure of the silica particles was studied by ^{29}Si solid-state NMR and Raman spectroscopy. The morphology was imaged by means of transmission electron microscopy (TEM), while the chemical structure of the (nano)composites was studied by Fourier transformed infrared spectroscopy (FTIR).

EXPERIMENTAL

Materials

Tetrahydrofuran (THF, p.a., ACROS Organics), hydrochloric acid (HCl, Merck, 37% p.a.), tetraethylorthosilicate (TEOS, Aldrich) were used as received.

PMMA, type PMMA-7N, was obtained from Evonik SE. The molar mass of PMMA-7N relative to PMMA calibration standards measured by size exclusion chromatography (SEC) was found to be $M_n = 48{,}600$ g/mol and $M_w = 93{,}400$ g/mol with a polydispersity $M_w/M_n = 1.84$.

Sample Preparation

Sol–Gel Process. Silica nanoparticles were prepared by an *in situ* sol–gel process in a solution of PMMA in THF with a verified procedure given by Silveira et al.[24] Thus, PMMA (10 wt % with respect to THF) was dissolved under stirring at 323 K in the appropriate amount of freshly distilled THF. The respective amount of TEOS/water and HCl (molar ratio 1/4/0.4 mol/mol/mol) was added under stirring at 313 K (procedure at pH = 1). To reach pH = 5, diluted HCl (0.01*M* HCl) was used maintaining the molar TEOS/water of 1/4 mol/mol. To achieve pH = 1, 1 mL of concentrated HCl was added in 50-mL reaction solution. The reaction solution was stirred at 313 K for 4 h. After that time, THF was removed using a rotary evaporator by distillation. The samples were dried at 313 K under reduced pressure for 6 h. Then the films were pressed in a melt press (Specac LOT with stability temperature controller 4000 series TM High with 500 -μm spacer rings) and subsequently annealed in a vacuum oven at 413 K for 8 h under reduced pressure to allow silica formation by polycondensation of the silanol groups.

Before all measurements (TGA, DSC, TSDC, and DRS), the hybrid samples were dried at 393 K under reduced pressure in a vacuum oven for 2 h and stored afterward in a closed dessicator over silica gel until use at the same day.

Preparation of Melt-Pressed Films. The PMMA/silica hybrid samples were pressed into circular films with diameters of 10–15 mm and thicknesses of about 50 μm by using a thermopress with a pressure of three tons at 443 K for 15–20 s.

Characterization Techniques

Differential Scanning Calorimetry. Differential scanning calorimetry (DSC) measurements were carried out by means of a DSC-Q-1000 (TA Instruments) with heating/cooling rate of 20 K/min in the temperature range of 193–473 K under nitrogen atmosphere.

Thermogravimetric Analysis. TGA measurements were performed in order to determine the correct content of silica introduced into the PMMA samples by sol–gel process. The measurements were done with Q-5000 (TA instruments) using a heating rate of 10 K/min in the temperature range from 303 to 1073 K under air. The residue obtained at 1073 K corresponds to the final silica content.

Transmission Electron Microscopy. Transmission electron microscopy (TEM) images were acquired from ultrathin sections of free-standing films (thickness about 80 nm), obtained by cryoultramicrotome EM/UC6 with cooling chamber FC6 (Leica) and diamond knife (Diatome) at 193 K by a TEM LIBRA 200 MC (Carl ZEISS, Germany) with an accelerating voltage of 200 kV.

ATR–FTIR Spectroscopy. The attenuated total reflectance–Fourier transformed infrared spectroscopy (ATR–FTIR) spectra were acquired with the Vertex-80v spectrometer (Bruker,

Table I. Preparation Conditions and Silica Contents of the PMMA/Silica Hybrid Samples Studied

Sample	Mass ratio polymer/ TEOS[a] (wt/wt)	pH	Calculated silica content (wt %)	Final silica content (wt %)
PMMA sol-gel[b]	100/0	1	0	0
PMMA/SiO_x-3.0%	90/10	5	4.0	3.0
PMMA/SiO_x-4.0%	70/30	1	11.0	4.0
PMMA/SiO_x-10.8%	70/30	5	11.0	10.8
PMMA/SiO_x-21.9%	50/50	5	22.3	21.9
SiO_x	0/100	1	100.0	100.0

[a]Composition in the reaction solution.
[b]PMMA control sample treated under the conditions of the sol-gel process.

Germany) in the wavelength range between 4000 and 600 cm^{-1}, the spectral resolution was 2 cm^{-1}, and 100 scans per spectrum were accumulated. The samples were measured with Golden Gate Diamond ATR unit (SPECAC, GB).

Raman Spectroscopy. The Raman measurements were done with the Raman microscope system HoloProbe5000 (Kaiser Optical, USA) in the range between 3500 and 150 cm^{-1} with a spectral resolution of 4 cm^{-1} and 200 scans per spectrum were coadded. The Raman system is equipped with a 785-nm diode laser, a holographic notch filter, and a CCD detector array. The laser power was 200 mW. Assignment of Q-groups to determine the degree of cross-linking: Q_2: 640 cm^{-1}; Q_3: 488 cm^{-1}; Q_4: 418 cm^{-1}. The bands were separated by peak fitting based on the Levenberg–Marquard method.[25]

^{29}Si Solid-State NMR. ^{29}Si MAS–NMR measurements were performed on a BRUKER Avance 500 NMR spectrometer (Bruker, Germany) operating at a resonance frequency of 99.36 MHz using a Bruker BL3.2 MAS probe head. The spinning frequency was 10 kHz. The ^{29}Si solid-state NMR spectra were acquired upon direct ^{29}Si polarization with ^{1}H decoupling (field strength 50 kHz), single 90° pulse of 4 μs, recycle delay of 500 s, and 500 repetitions. The ^{29}Si chemical shifts were referenced to TMS using Q_8M_8 as an external standard, which gives a Si(—CH_3)$_3$ signal at 12.6 ppm. The spectra were fitted using Dmfit.[26] Assignment of Q-groups to determine the degree of cross-linking: Q_2: −91 ppm; Q_3: −100 ppm; Q_4: −110 ppm. The calculation of the degree of cross-linking D(Q) was accomplished according to Ref. 26.

$$D(Q) = \frac{1Q_1 + 2Q_2 + 3Q_3 + 4Q_4}{4} \quad (1)$$

Thermally Stimulated Depolarization Currents

Thermally stimulated depolarization current (TSDC) is a special dielectric technique working in the temperature domain. It is a sensitive dc method frequently used for the fast characterization of materials through their dielectrically active relaxation phenomena. The main advantage of the method is the high-resolving power arising from its low-equivalent frequency (10^{-4} – 10^{-2} Hz).[28–30] By this technique, the sample was inserted between the brass plates of a capacitor (10–15 mm in diameter) placed in a Novocontrol sample cell and polarized by an electrostatic field E_p (∼100 V/mm) with a voltage source at polarization temperature T_p = 383 K for time t_p = 5 min. With the field still applied, the sample was cooled down to 123 K (cooling rate 10 K/min), sufficiently low to prevent depolarization by thermal fluctuations. Then the sample was short-circuited and heated up to 423 K at a constant heating rate b = 3 K/min. A discharge current was generated during heating and measured as a function of temperature with a sensitive programmable Keithley 617 electrometer. Temperature control was achieved by means of a Novocontrol Quatro cryosystem. The samples were circular films of diameter 10–15 mm and thickness of about 60 μm.

Dielectric Relaxation Spectroscopy. For dielectric relaxation spectroscopy measurements (DRS),[31] the samples (similar to those used for TSDC measurements) are placed between the plates of a capacitor, and an alternate voltage is applied in a Novocontrol sample cell. The complex permittivity $\varepsilon^* = \varepsilon' - i\varepsilon''$ is recorded isothermally as a function of frequency in the range of 10^{-1} – 10^6 Hz at temperatures 123–363 K in steps of 10 K in order to follow local relaxations and at temperatures 363–423 K in steps of 5 K in order to follow the segmental dynamics (dynamic glass transition), which has a stronger temperature dependence. ε^* is recorded using a Novocontrol Alpha Analyzer, while the temperature is controlled to better than 0.5 K with a Novocontrol Quatro cryosystem.

RESULTS AND DISCUSSION

Structure of the PMMA/Silica Hybrids

The poly(methyl methacrylate) (PMMA) used in the experiments discussed here did not contain functional groups and resulted therefore in silica hybrids without covalent linkage between the polymer matrix and silica nanoparticles ("class I hybrids" according to Sanchez et al.[1]). Thus, hybrids with a clearly defined state should be obtained. Covalent linkages are excluded, and interactions between organic and inorganic phase can only occur by hydrogen bonds between the Si—OH terminal groups of the silica and carbonyl groups of PMMA as well as via dispersive forces. Table I summarizes the reaction conditions as well as the silica contents of the PMMA/silica hybrids.

It can be noted that the final silica contents obtained experimentally by TGA measurements were mostly in the range of the calculated ones showing that TEOS was completely converted to silica under the given conditions. The pH values used for the reactions and the acid catalysis should lead to hybrids with a linear, less-branched, and open silica network or silica

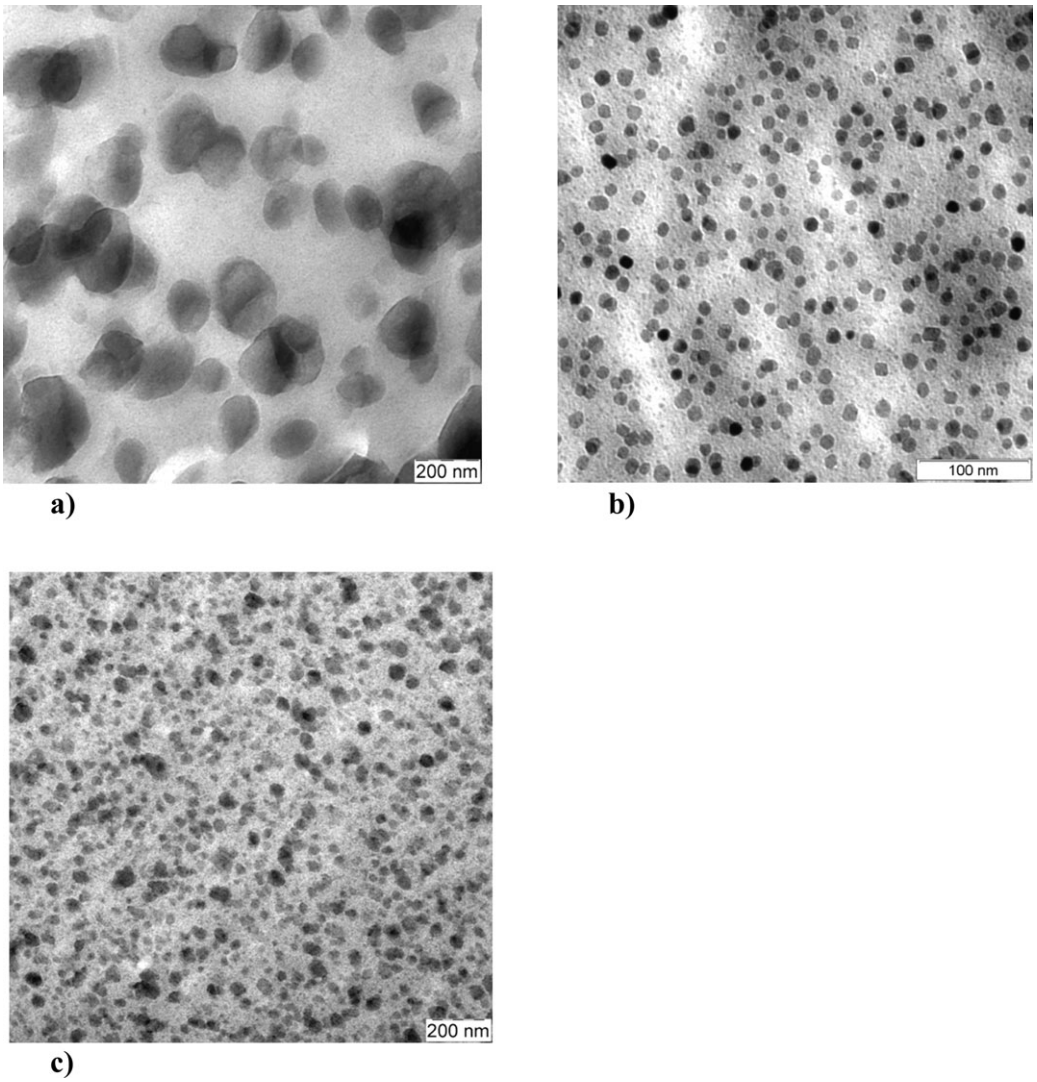

Figure 1. TEM images of PMMA nanocomposites with different amount of silica: (a) PMMA/SiO_x-3 wt % (particle diameter: 142.7 ± 33.0 nm); (b) PMMA/SiO_x-10.8 wt % (particle diameter: 12.9 ± 2.1 nm); (c) PMMA/SiO_x-21.9 wt % (particle diameter: 46.8 ± 11.1 nm).

nanoparticles.[32] The pH should mainly influence the reaction rate: faster hydrolysis at pH = 1 should result in agglomerated particles, while the reaction performed at pH = 5 should yield a slow hydrolysis and nanoscale silica particles. Indeed, TEM images revealed the formation of silica nanoparticles within the PMMA matrix polymer, as illustrated in Figure 1. In samples with lower content of silica (2.9 wt %), the generated particles are the largest (142 nm), increasing the concentration that reduces the average diameter below 50 nm.

In a next step, the internal structure of the silica obtained in the sol–gel process was evaluated in order to verify that it is comparable for different compositions. This is an important presumption for the comparison of polymer dynamics of the hybrids. The silica structure can be described by the degree of condensation of the SiO_x network, which is expressed by the number (i.e., concentration) of different terminal groups. Depending on this, Q_1 (three terminal OH-groups), Q_2 (two terminal OH-groups), Q_3 (one terminal OH-group), and Q_4 (no terminal OH-group) groups are differentiated.[33] Q_1 is the basic unit having the lowest degree of condensation. The content of Q-groups is determined with methods allowing to identify Si atoms in different environment. Particularly useful methods are ^{29}Si solid-state NMR spectroscopy[27] as well as Raman spectroscopy.[34,35] Both methods were used in this study to quantify the silica network structure. As the reaction conditions (TEOS/water molar ratio, solvent, temperature, see "Experimental" section) were kept constant, a similar structure of the silica networks in hybrid samples with different concentration was assumed. The results are summarized in Table II and show a comparable degree of cross-linking obtained with both methods in all hybrid samples with a degree value between 76 and 84%. Thus the silica particles generated by the used procedure are highly cross-linked.

DSC and TSDC

For a proper investigation of the effects of silica generated by sol–gel processes on the thermal transitions and dynamics of PMMA, it is crucial to examine first as to whether the chemical procedure of the sol–gel reaction forming silica particles within the PMMA matrix is affecting the properties of neat PMMA.

Table II. Characterization of PMMA/Silica Hybrids by ^{29}Si Solid-State NMR and Raman Spectroscopy

		^{29}Si-NMR spectroscopy				Raman spectroscopy			
Sample	SiO_x content (wt %)	Q_2 (%)	Q_3 (%)	Q_4 (%)	D (Q)	Q_2 (%)	Q_3 (%)	Q_4 (%)	D (Q)
PMMA/SiO_x-10.8%	10.8	23	47	30	77	21	61	18	74
PMMA/SiO_x-21.9%	21.9	8	50	42	81	2	66	32	83
SiO_x	100	5	42	53	86	8	60	32	81

Therefore, the starting PMMA as obtained from the supplier and a sample of PMMA, which was treated in the same manner as the sol–gel procedure was carried out but without silica precursor (final content 0 wt % SiO_x), were compared. It has to be pointed out that all PMMA/silica hybrid samples have to be dried carefully right before all measurements, because these hybrids contain water probably within pores, which may significantly alter the results, in particular the position of the glass transition. This is illustrated by the decrease of the glass transition temperature (T_g) of the starting PMMA material after the sol–gel control procedure (Figure 2, see below). According to SEC results, this drop is not caused by any decrease of molar mass caused by the treatment.

Figure 2 shows the comparative DSC curves of the second heating run to erase thermal history for the starting PMMA as obtained from the supplier and the sol–gel-treated PMMA sample in the region of the glass transition. It appears that the sol–gel procedure results in a decrease in the glass transition temperature (T_g). As mentioned earlier, SEC results ruled out the possibility that this decrease is caused by a decrease of molar mass, as it might be supposed. The reason for the T_g decrease is rather clear, because many different aspects, such as remaining water molecules strongly adsorbed at the outer silanol groups that increase the free volume due to loosened molecular packing of the chains (plasticization) or effect on the molecular profile of the chains by remaining solvent (THF), may contribute.[36–38] The effort to remove these plasticizing factors by increasing the annealing temperature from 353 to 413 K caused side effects on the morphology. Especially, the increase in the temperature intensified the molecular mobility of the polymer chains; thus, the silica particles proximity decreased and they formed aggregates. Thus, for the study of the effect of the silica nanoparticles on molecular mobility and properties of the matrix, the sample of PMMA that has undergone the sol–gel procedure (from now on referred to as PMMA sol–gel) has been chosen as reference in the following. Table III shows the DSC results for all nanocomposite samples and also for the reference sample (PMMA sol–gel, 0 wt % SiO_x). A systematic increase of about 2–6 K of the T_g is observed for increasing silica content (Figure 3). This increase tends to saturate in a constant temperature for high-silica content (above 20 wt % SiO_x). Also, a decrease, but not a systematic one, is observed for Δc_p values for increasing silica content (Table III), where Δc_p is obtained by DSC as the heat-capacity jump during the glass transition. In other works, it has been shown that the Δc_p decrease may be attributed to an immobilized fraction of the amorphous polymer (rigid amorphous fraction; RAF) around the nanoparticles that does not contribute to the glass transition equally to the bulk polymer.[7,39] First, the normalized to the polymer fraction Δc_p value is obtained according to eq. (1), and the results are shown in Table I.

$$\Delta c_{p,\mathrm{norm}} = \frac{\Delta c_p}{x_{\mathrm{poly}}} \tag{2}$$

where $x_{\mathrm{poly}} = 1 - x_{\mathrm{filler}}$ is the polymer fraction.

By using the $\Delta c_{p,\mathrm{norm}}$ values obtained by eq. (2), a calculation of the RAF of the polymer can be made according to (Table III):

$$x_{\mathrm{im}} = 1 - \frac{\Delta c_{p,\mathrm{norm}}}{\Delta c_{p,\mathrm{pure}}} \tag{3}$$

where $\Delta c_{p,\ \mathrm{norm}}$ and $\Delta c_{p,\ \mathrm{pure}}$ refer to normalized heat-capacity increments at the glass transition for the nanocomposite materials and for the pure polymer, respectively. The values obtained decrease for increasing silica content, but not in a systematic way. This nonsystematic decrease may be the result of significant changes in the quality of particles dispersion (i.e., formation of aggregates) for increasing silica content. By studying more compositions in the future, we should be able to complete the intermediate region and produce a more complete picture, and experiments are in progress in this direction. In a very

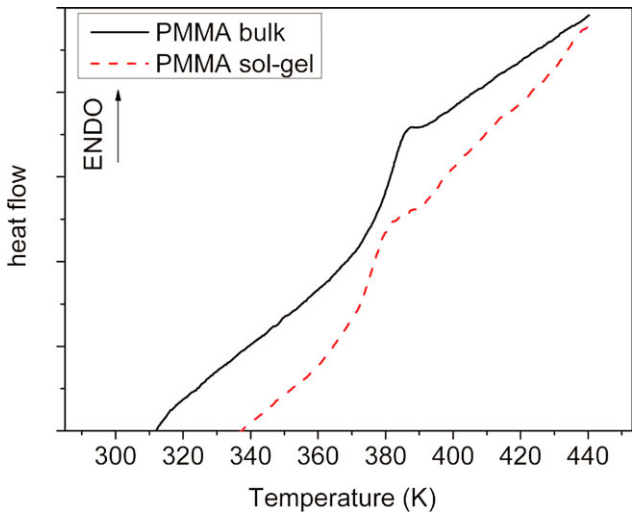

Figure 2. DSC thermogram in the region of glass transition for bulk PMMA and PMMA after treatment under sol–gel conditions. [Color figure can be viewed in the online issue, which is available at wileyonlinelibrary.com.]

Table III. Parameters of Calorimetric Glass Transition [Glass Transition Temperature T_g, Normalized Heat Capacity Increment $\Delta c_{p,\,norm}$, Fraction of Immobilized Polymer x_{im} Calculated According to eq. (3), Difference in Glass Transition Between Sample and Reference ΔT_g] as Measured by DSC and of the Segmental α Relaxation (Peak Temperature T_α, Difference in Peak Temperature Between Sample and Reference ΔT_α) as Measured by TSDC

	DSC				TSDC	
Sample	T_g (K)	$\Delta c_{p,\,norm}$ (J/gK)	x_{im}	ΔT_g (K)	T_α (K)	ΔT_α (K)
PMMA sol-gel	379	0.39	0.00	0	369	0
PMMA/SiO_x-3.0	383	0.29	0.26	4	375	6
PMMA/SiO_x-4.0%	382	0.34	0.13	3	377	8
PMMA/SiO_x-21.9%	385	0.27	0.31	6	379	10

systematic study of PMMA/silica nanocomposites, prepared by melt-mixing, Sargsyan et al.[7] have linked the decrease of the heat-capacity jump to the existence of an immobilized fraction of the polymer, which does not contribute to the glass transition. It is interesting that the same work discussed that this fraction of the polymer is not observed to devitrify even at very high temperatures. This picture seems to change qualitatively after using dielectric techniques,[40,41] which depict a different behavior. The dielectric relaxation linked to the glass transition is directly observed as a strong peak, although it exhibits longer relaxation times (two to three orders of magnitude). So, the picture about the presence of an immobilized fraction of polymer should not be extracted only from the DSC data, but it should be taken into account the fact that the nanoparticles may affect the segmental dynamics in a more complex way. Either observing a simple shift of T_g of the bulk material or interpreting a complete immobilization of a fraction of polymer segments could be only one part of the picture. To complete the picture about the silica influence on the molecular mobility, we should examine the data obtained with dielectric techniques first.

The analysis of the TSDC spectra shows a strong peak for all samples attributed to the dynamic glass transition at a different temperature (T_α) for each sample. The temperature T_α of the segmental relaxation peak has been found to be in good agreement with the calorimetric glass transition temperature and has been proved to be a good measure of the T_g due to similar time scales of the experiments.[30] Therefore, the results concerning the temperature of the glass transition from TSDC and DSC are summarized together in Table II. Moreover, these combined data, in the form of $\Delta T_g = T_{g,comp} - T_{g,ref}$ (where $T_{g,ref}$ is the glass transition temperature of the PMMA sol–gel, 0 wt %) from DSC (T_g) and TSDC (T_α), are plotted in Figure 3 against the silica content. Both methods detect the same behavior, an increase of T_g for increasing silica content with a trend to saturate at high-silica contents, above 20 wt %. The increase of T_g can be assigned to hydrogen bonds occurring between surface OH groups of silica particles and the ester side group of the PMMA chain. The FTIR spectra that depict a possible OH bonding also lead to this direction. The saturation can be explained as a result of the aggregation of the silica particles, because the formation of aggregates limits the number of the interfaces between polymer and filler.[7] Therefore, the effect of the silica is suppressed, and it is no longer linearly dependent on the filler content. Even though several works have reported an increase of the glass transition temperature due to the interactions between PMMA and silica particles, few of them have reported the saturation of this increase.[7] One possible explanation to explain such a discrepancy may reside on the fact that most of works concentrate on low-silica content systems (below 10 wt %), where the aggregation level is sufficiently low to avoid significant effect on the volume to surface ratio of the nanoparticles. Results obtained for another acrylate/silica system (PHEA/silica) produced by sol–gel method[42,43] also imply a change of behavior at high-filler fraction; for values above 10–15 wt %, the effect of the filler is magnified, most probably due to the formation of a continuous inorganic network, which interacts physically with the polymer chains.

Dielectric Relaxation Spectroscopy

Figure 4 shows representative dielectric loss (ε'') spectra recorded with the material with 3 wt % SiO_x at selected temperatures. The temperature dependence of the imaginary part of dielectric permittivity (dielectric loss) ε'' is presented versus frequency for selected temperatures. Three dielectric relaxation peaks are observed in different temperature regions: γ relaxation

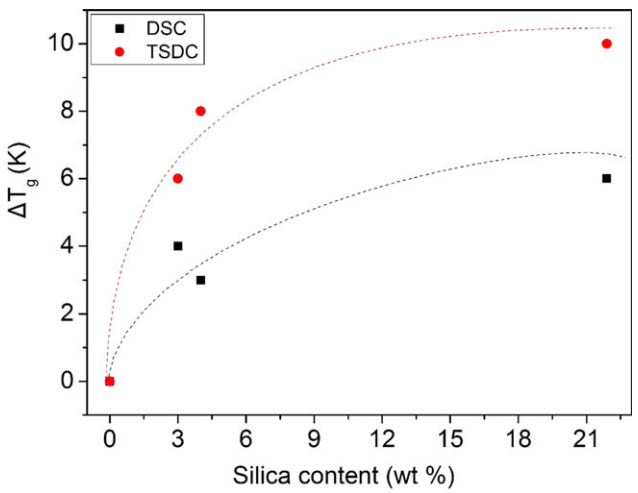

Figure 3. Change of glass transition temperature of the PMMA phase ($\Delta T_g = T_{g,\,PMMA/silica} - T_{g,\,PMMA\ sol-gel}$), in the different PMMA/silica hybrids as function of filler content, the T_g of the reference PMMA sol–gel was 378 K. [Color figure can be viewed in the online issue, which is available at wileyonlinelibrary.com.]

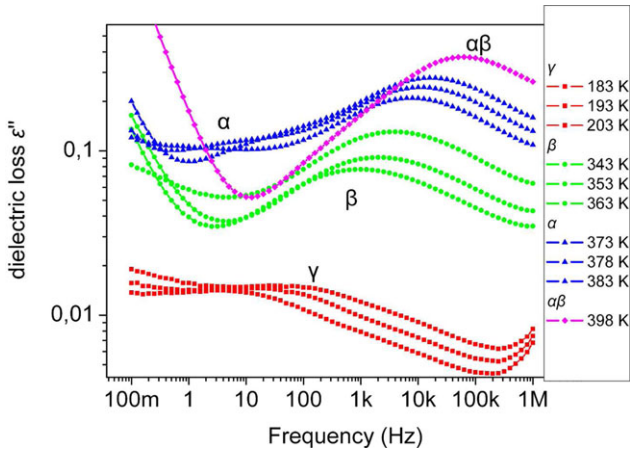

Figure 4. Representative dielectric relaxation spectroscopy spectra for sample with 3% SiO_x of imaginary part of dielectric permittivity ε'' as a function of frequency f for selected temperatures. Three dielectric relaxations (γ, β, α) are observed in order of increasing temperature, plus the complex $\alpha\beta$ relaxation at high temperatures. [Color figure can be viewed in the online issue, which is available at wileyonlinelibrary.com.]

(163–253 K), β relaxation (263–393 K), and α relaxation (373–393 K) in order of increasing temperature. Each relaxation is attributed to the molecular motion of a different part of the polymer chain. The γ and β relaxations originate from local motions of two different side groups of the chain; therefore, they are characterized as secondary relaxations. The first is born from the rotation of the $-CH_3$ side group around its bond to the backbone of the polymer, while the latter relaxation from the rotation of the $COOCH_3$ side group around the C=O bonds to the main part of the chain.[44] In some works, the γ relaxation is tentatively associated with the presence of traces of water in the sample,[45] while others separate the existence of the relaxation from the presence of water.[23]

The α relaxation (Figure 4), attributed to the dynamic glass transition, is the dielectric fingerprint of the glass transition and originates from the co-operative motion of large fragments of the chain backbone and can be observed at ~5 Hz for temperature 378 K. In the region of high temperatures and frequencies, a merging of the α and β relaxation to a complex $\alpha\beta$ relaxation (393–418 K) is observed, a typical behavior for PMMA.[46] This observation is very important for the study of the PMMA, because it reveals that the β relaxation has a partially co-operative character; therefore, several studies focused on this temperature region.[22,46–50] This kind of secondary relaxation with a co-operative character is known as Johari–Goldstein relaxation[51] (JG β-relaxation here) and has been observed in many different systems under various conditions.[52]

The β relaxation (Figure 4) is the dominant relaxation in the spectrum, because the molecular group that creates it has a very strong dipole moment; therefore, the material relaxes mainly through this relaxation. We like to stress here that the α relaxation is very difficult to be detected in isothermal plots for two reasons. The first is that the α relaxation of PMMA is very weak and broad, that is, covers a very large range of frequencies (very broad distribution of relaxation times) and thus is observed in only a limited temperature region. The second is the presence of strong conductivity contribution in the region of low frequencies at temperatures above T_g where the α relaxation is expected, which is a typical behavior for acrylates–methacrylates.[43,50,53,54] The observed conductivity (Figure 4, low frequencies region) originates either from charges trapped between the interfaces of the matrix and the filler or trapped large molecules of solvent.

To clarify whether the sol–gel procedure had any effect on the secondary β relaxation, the comparative plot of bulk PMMA and PMMA sol–gel is presented in Figure 5. No apparent difference can be observed; neither for the shape nor for the position of the peak. A strong signal of conductivity is observed for the PMMA sol–gel as a steep slope at low frequencies. This effect is probably caused by remaining solvent molecules or water molecules. The emergence of the conductivity can be the reason of the small overall increase of the response of this sample compared to the bulk PMMA. Similar results have also been obtained for γ relaxation. Therefore, it can be assumed that the chemical procedure during the preparation of the samples had no effect on the secondary relaxations of the matrix. Nevertheless, the sample of PMMA sol–gel will be again used as a reference for the nanocomposite samples, because an effect on the α relaxation is expected according to the increase of the T_g obtained from DSC and TSDC.

The study of the effect of silica nanoparticles on the matrix begins with Figure 6, where a comparative dielectric relaxation spectroscopy (DRS) diagram in the region of β relaxation is presented. No systematic change of the peak frequency (time scale) can be detected for increasing silica content. By comparing the overall response of each sample's spectrum, small changes can be detected. This behavior is not systematic and, possibly, is related to experimental inaccuracy in the estimation of the thickness of the sample. This observation should be highlighted, because the study of the β relaxation of PMMA has been repeatedly linked with the study of the physical aging.

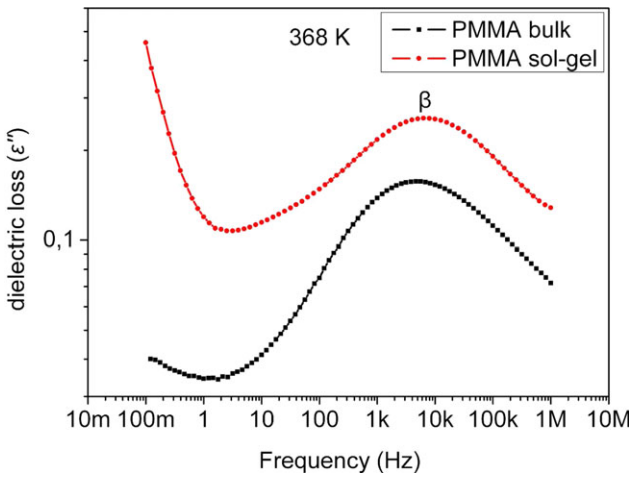

Figure 5. Comparative isothermal plot of dielectric loss ε'' versus frequency f for bulk PMMA and PMMA sol–gel at 368 K. [Color figure can be viewed in the online issue, which is available at wileyonlinelibrary.com.]

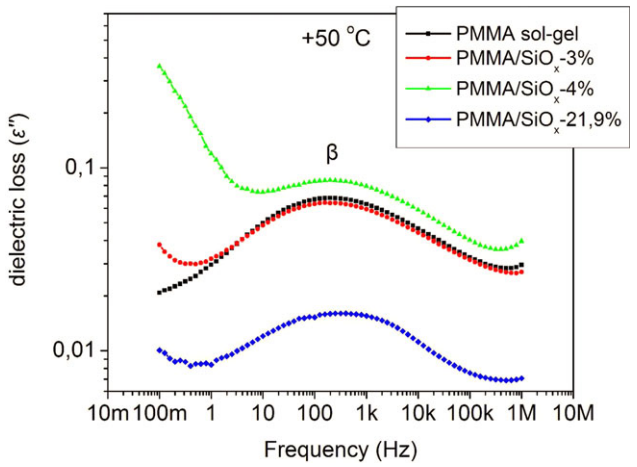

Figure 6. Comparative isothermal plot of the dielectric loss ε'' versus frequency f at 323 K for all samples. [Color figure can be viewed in the online issue, which is available at wileyonlinelibrary.com.]

Because the physical aging is a very crucial phenomenon for the mechanical properties of the polymer deep in the glassy state, it is important to examine how these results can be combined with previous works. Priestley et al.[22] in systems of PMMA/silica nanocomposites obtained by melt-mixing have observed a systematic and significant decrease in the dielectric strength of the β relaxation for increasing silica content, even at very low-silica content. A similar decrease has also been observed by Casalini and Roland[55] during physical aging experiments in low-molecular weight neat PMMA and has been attributed to the structural confinement introduced by the evolution of the physical aging. Therefore, the effect of the silica particles on the β relaxation has been assigned to the suppression of the physical aging in PMMA as the decrease of the dielectric strength of the β relaxation is supposed to reflect the reduction of the mobility of the side ester group, which is strongly related to the segmental mobility of the main chain as a JG β relaxation. An interpretation could be that the presence of the filler restricts the general mobility of the backbone of the chain, and the structural relaxation linked to the physical aging is also suppressed. Similar observations have been made by Boucher et al.[56,57] also in nanocomposite systems of PMMA/silica obtained by *in situ* polymerization of methyl–methacrylate in the presence of silica nanoparticles. Nevertheless, in other works,[23] where samples were produced in the same way as the samples presented here, no apparent change in the β relaxation is observed. Same results have been obtained from dielectric measurements (not yet published) on the samples of Sarsgsyan et al.,[7] where despite the systematic increase of the T_g, no effect on the β relaxation has been observed at any silica content. Experiments in progress on different PMMA/silica materials obtained by a different preparation method show a strong effect of the filler on the β mode of the polymer, as has also been reported by Kalogeras.[58] These results will be reported in future work. An assumption about the origin of this disagreement could be the different preparation routes for each system. It has been proved that according to the preparation procedure that is followed, different final properties are obtained for silica nanocomposites.[18,24] Li et al.[23] have studied PMMA/silica nanocomposites obtained by sol–gel technique, where no difference of the β relaxation has been detected for increasing silica content. The results we present here have been produced in a similar way (similar specifications about the preparation procedure), and they indicate that no change of the β relaxation is caused by the silica presence within the experimental error. So, it is safe to assume that the similarity between our results and the results of Li et al.[23] is due to the similar structural profile of the samples.

A more general survey of the dielectric behavior of the samples can be obtained through the Arrhenius plot (dielectric map) in Figure 7, where the frequency of maximum of ε'' is plotted against reciprocal temperature. This kind of depiction can be very revealing about the temperature/timescale behavior of each relaxation. In the same plot, the temperature points obtained by DSC and TSDC have been included at the equivalent frequencies of ~0.01 Hz[30] and 1.6 mHz,[6] respectively. Besides the data obtained from the simple isothermal depiction, data obtained from isochronal plots were also used. In these plots, dielectric loss data (ε'') obtained isothermally at various frequencies have been replotted as a function of temperature. We will not present such plots, but they were constructed and used in order to enrich the Arrhenius plot, especially in the region of the α relaxation. This kind of data depiction is a tool often used.[59–61] The analysis for the isothermal data has been made by reading the frequency maxima for each relaxation for all measured temperatures, while the isochronal data are obtained the same way but reading the temperature maxima. Plurality of the relaxations on one hand and strong overlap between them on the other made it difficult to obtain reliable results through a fitting procedure with model function (e.g. like that performed in Refs. 45, 49, and 53).

All three relaxations are observed in their respective temperature region. An interesting point in the Arrhenius plot is the region

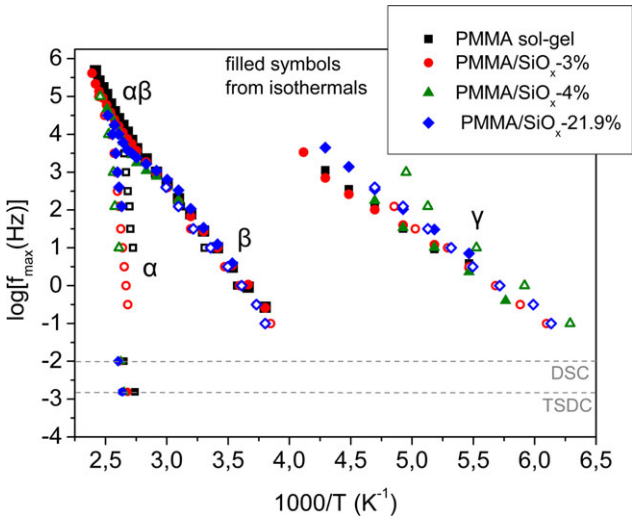

Figure 7. Arrhenius plot (dielectric map) for all samples. The data from DSC and TSDC have been included at the equivalent frequencies. Data obtained from isothermal (filled symbols) and isochronal (blank symbols) plots are presented. [Color figure can be viewed in the online issue, which is available at wileyonlinelibrary.com.]

Table IV. Activation Parameters for the γ, β, and αβ Processes

	γ process		β process		αβ process	
Sample	logf_0	E_a (kJ/mol)	logf_0	E_a (kJ/mol)	logf_0	E_a (kJ/mol)
PMMA sol-gel	13.1	44	14.0	79	19.0	115
PMMA/SiO_x-3.0	13.5	46	13.0	68	19.5	113
PMMA/SiO_x-4.0%	13.0	39	14.3	76	20.2	116
PMMA/SiO_x-21.9%	12.5	44	15.0	81	19.7	121

The fitting was made with eq. (4).

of the merging of α and β relaxations in a complex αβ, as mentioned earlier.[17,46–48] This complex process is faster than the β relaxation (smaller slope) and slower than the α relaxation (bigger slope). Also, the αβ relaxation, even if it is attributed to the rubber state of the polymer above T_g and it is originated from segmental molecular motions, is better described by an Arrhenius equation [eq. (4)] rather than a Vogel–Tamman–Fulcher–Hesse (VTFH) equation [eq. (5)].[47] Such behavior is typical for secondary relaxations and not for segmental processes. The equations used for describing the dependence of each relaxation from the temperature are the Arrhenius equation:

$$f = f_0 \exp\left(-\frac{E_a}{kT}\right) \quad (4)$$

where f_0 is the proexponential factor, k the Boltzmann constant, E_a the activation energy of the mechanism, and the VTFH equation.

$$f = f_0 \exp\left(-\frac{B}{T - T_0}\right) \quad (5)$$

where B, f_0, and T_0 (Vogel temperature) are the constants independent of the temperature.[62]

By applying these two equations to the data of the dielectric map, a fitting can be made in order to obtain an estimation about the activation energy of each process.

Before we proceed to calculations of VTFH and Arrhenius parameters by fitting eqs. (4) and (5) to the data, we make some qualitative observations in a "less analysis" approach. Starting with γ relaxation at low temperatures, a significant scattering of the data can be observed. In general, the behavior of the relaxation is not affected systematically by the presence of the silica particles. The scattering can be attributed to the influence of the water molecules, because there are strong indications that some remaining water may not have been removed by the annealing procedure. Such indications are the decrease of the T_g of the neat PMMA sol–gel in comparison with that of the bulk PMMA (Figure 2) and the steep increase of the signal at low frequencies in the dielectric measurements (Figures 5 and 6).

Regarding the β relaxation, no systematic change of the time scale can be detected due to the presence of silica. By following the evolution of the β relaxation toward the high-frequencies region, a change of the slope can be detected at about 358 K. This change reflects the beginning of the merging of the β with the α relaxations, which is a typical behavior for PMMA and acrylates in general.[17,46–48,63] The observation of this change verifies the partially co-operative character of the β relaxation, which is strongly affected by the forthcoming segmental dynamics. Another point that should be considered is the second change of the slope, observed at lower temperatures (at about 303 K) mainly for the nanocomposites. To the best of our knowledge, there is no similar report in the bibliography. A possible explanation about this odd behavior could be the influence of the silica particles on the homogeneity of the intramolecular environment. Nanoparticles may have disturbed in their vicinity, the environment of the polymer chains by affecting the molecular mobility assigned to the high-temperature region of the β relaxation. Because the β relaxation has been proven to be partially cooperative, the effect of silica particles on the segmental dynamics could be mirrored in the β relaxation more intensively near the beginning of the merging region than at lower temperatures. This explanation is supported by the fact that the change of the slope is more intense for the sample with the high-silica content (blue rhombus in Figure 7).

In the region of the glass transition temperature (~373 K), the α relaxation enters the measurement window, and, through its evolution, it merges with the β relaxation into a complex αβ. The dielectric data for the α mode are in good agreement with the data obtained by the TSDC and DSC for T_α and T_g, respectively. Comparing the samples with different silica content, a shift of the relaxation to higher temperatures–lower frequencies with increasing SiO_x content is observed in agreement with TSDC and DSC. Also, by following the behavior of the αβ

Table V. Activation Parameters for the α Process

	α process		
Sample	logf_0	B	T_o (K)
PMMA sol-gel	13.0	1053	329
PMMA/SiO_x-3.0%	13.0	1062	344
PMMA/SiO_x-4.0%	13.0	1275	332
PMMA/SiO_x-21.9%	13.0	1579	315

The value of logf_0 was fixed to 13.0. The fitting was made with eq. (5).

relaxation, a similar conclusion can be extracted, because the relaxation maximum shifts to higher temperatures for increasing silica content. In general, the presence of silica results in a slowing down of the segmental dynamics of the matrix. This is expressed both through the effect on α and αβ relaxation.

To quantify the temperature time-scale dependence in terms of eqs. (4) and (5), the Arrhenius equation [eq. (4)] has been fitted to data for γ, β, αβ, and results obtained for pre-exponential factor (f_0) and activation energy (E_{act}) are reported in Table IV. The values obtained for both γ and β relaxations show no systematic change with increasing silica content. This comes in agreement with the previous conclusions from the analysis of the DRS spectra and the qualitative analysis of the Arrhenius plot. The E_{act} values obtained for both relaxations are in good agreement with the results obtained by various groups.[23,57,63,64] The discussion about the origin of the γ relaxation is still open, because some groups report similar to our values for E_{act} to be the activation energy of a pure molecular motion of a side-chain group,[23] while others are associating this E_{act} value to a molecular motion triggered by water molecules.[58] By comparing the values for the nanocomposites, no significant change of the E_{act} or the f_0 can be observed. Again, the picture of unaffected by silica secondary relaxations is enhanced from another aspect.

The VTFH equation [eq. (5)] was fitted to the α-relaxation data. To reduce parameters for evaluation, we followed common praxis and fixed f_0 to the phonon value $f_0 = 10^{14}$ Hz.[31] Results obtained for B and T_0 are reported in Table V. An increase of the B value is observed for increasing silica content, while the T_0 does not show any systematic change. In general, the values obtained here are in good agreement with the reported values in other works.[46,48,50,54] It is still not safe to draw definitive conclusions at this point, because the data for this analysis have been drawn from a limited number of experiments. The study of a more complete series of samples from the same system will enhance the statistical plurality of the results and will lead to more concrete results regarding the fitting analysis of the α relaxation. Nevertheless, the picture of affected segmental dynamics by the silica presence, which until now is obtained by the other methods, is enhanced here by the findings regarding the α relaxation.

CONCLUSIONS

PMMA nanocomposites with silica nanoparticles (SiO_x) were synthesized via sol–gel method and characterized by various techniques. The presence of particles with size in the range of 10–100 nm was determined by TEM. Solid-state NMR and Raman spectroscopy revealed the formation of an inorganic network from the nanoparticles with a high degree of crosslinking (i.e., 76–84%). To elucidate the impact of the filler on the molecular mobility of the polymer matrix, different methods were used; DSC and TSDC measurements showed an increase of the glass transition temperature with increasing silica content. This increase saturates for high-silica content (above ~20 wt %), most probably due to the aggregation of the particles. Also, broadband DRS was used as a tool to study the full range of molecular motions of the PMMA in the presence of the SiO_x particles. Although the secondary relaxations (β, γ) related to the motions of the side chains are not affected for any weight fraction of SiO_x, the primary relaxation (α) of the segmental dynamics is affected for increasing silica content. Namely, a slowing down of the α relaxation is observed, which reflects the restriction of molecular mobility of the matrix induced by the silica. One possible explanation could reside on the formation of hydrogen-bonding interactions between the silica surface OH groups and the ester side group of the polymer chain. This explanation is supported by the increase in the mobility restriction with increasing silica content; that is, the increase of the interfaces gives rise to stronger interaction.

ACKNOWLEDGMENTS

Financial support by Greek and German Academic Exchange Service (Ikyda program) is gratefully acknowledged. The authors thank Dr. Sotiria Kripotou for fruitful discussions during the preparation of this manuscript.

REFERENCES

1. Sanchez, C.; Julian, B.; Belleville, P.; Popall, M. *J. Mater. Chem.* **2005**, *15*, 3559.
2. Sperling, L. H. Introduction to Physical Polymer Science; Wiley: New York, **2006**.
3. Mark, J. *Polym. Eng. Sci.* **1996**, *36*, 2905.
4. Micusik, M.; Omastova, M.; Krupa, I.; Prokes, J.; Pissis, P.; Logakis, E.; Pandis, C.; Poetchke, P.; Pionteck, J. *J. Appl. Polym. Sci.* **2009**, *113*, 2536.
5. Coleman, J. N.; Cadek, M.; Ryan, K. P.; Fonseca, A.; Nagy, J. B.; Blau, W. J.; Ferreira, M. S. *Polymer* **2005**, *46*, 4144.
6. Fragiadakis, D.; Pissis, P. *J. Non-Cryst. Sol.* **2007**, *353*, 4344.
7. Sargsyan, A.; Tonoyan, A.; Davtyan, S.; Schick, C. *Eur. Polym. J.* **2007**, *43*, 3113.
8. Klonos, P.; Panagopoulou, A.; Kyritsis, A.; Bokobza, L.; Pissis, P. *J. Non-Cryst. Sol.* **2011**, *357*, 610.
9. Privalko, V. P.; Titov, G. V. *Polym. Sci. USSR* **1978**, *21*, 380.
10. Liu, X.; Wu, Q. *Polymer* **2001**, *42*, 10013.
11. Bershtein, V. A.; Egorova, L. M.; Yakushev, P. M.; Pissis, P.; Sysel, P.; Brozova, L. *J. Polym. Sci. Part B: Polym. Phys.* **2002**, *40*, 105.
12. Ash, B. J.; Schadler, L. S.; Siegel, R. W. *Matter. Lett.* **2002**, *55*, 83.
13. Paul, D. R.; Robenson, L. M. *Polymer* **2008**, *49*, 3187.
14. Träxler, M.; Schäfer, M.; Blas, R.; Albrecht, K. *Kunststoffe Plast. Eur.* **2005**, *95*, 114.
15. Gross, S.; Camozzo, D.; Di Noto, V.; Armelao, L.; Tondello, E. *Eur. Polym. J.* **2007**, *43*, 673.
16. Lin, R.; Chen, B.; Chen, G.; Wu, J.; Chiu, H.; Suen, S. *J. Membr. Sci.* **2009**, *326*, 117.
17. Pandis, C.; Logakis, E.; Kyritsis, A.; Pissis, P.; Vodnik, V. V.; Dzunuzovic, E.; Nedeljkovic, J. M.; Hernandez, J. C. R.; Ribelles, J. L. G. *Eur. Polym. J.* **2011**, *47*, 1514.

18. Wen, J. *Encyclopedia of Materials: Science and Technology*, Elsevier, **2001**; p 7610.
19. Parker, K.; Schneider, R. T.; Siegel, R. W.; Osizik, R.; Cabanelas, J. C.; Serrano, B.; Antonelli, C.; Baselga, J. *Polymer* **2010**, *51*, 4891.
20. Chan, C. K.; Peng, S. L.; Chu, I. M.; Ni, S. C. *Polymer* **2001**, *42*, 4189.
21. Boucher, V. G.; Cangialosi, D.; Alegria, A.; Colmenero, J.; Gonzalez-Irun, J.; Liz-Marzan, L. M. *J. Non-Cryst. Sol.* **2011**, *357*, 605.
22. Priestley, R. D.; Rittigstein, P.; Broadbelt, L. J.; Fukao, K.; Torkelson, J. M. *J. Phys.: Condens. Matter* **2007**, *19*, 205120.
23. Li, C.; Wu, J.; Zhao, J.; Zhao, D.; Fan, Q. *Eur. Polym. J.* **2004**, 40, 1807.
24. Silveira, K. F.; Yoshida, I. V.; Nunes, S. P. *Polymer* **1995**, *36*, 1425.
25. Marquardt, D. W. *J. Soc. Ind. Appl. Math.* **1963**, *11*, 431.
26. Massiot, D.; Fayon, F.; Capron, M.; King, I.; LeCalve, S.; Alonso, B.; Durand, J.-O.; Bujoli, B.; Gan, Z.; Hoatson, G. *Magn. Reson. Chem.* **2002**, *40*, 70.
27. Pouxviel, J. C.; Boilot, J. P.; Beloeil, J. C.; Lallemand, J. Y. *J. Non-Cryst. Sol.* **1987**, *89*, 345.
28. Brauenlich, P. Stimulated Relaxation in Solids; Springer: New York, **1979**.
29. Vandershueren, J.; Gasiot, J. In: Topics in Applied Physics; Sessler, G. M., Ed.; Springer: Berlin, **1980**.
30. Vatalis, A. S.; Kanapitsas, A.; Delides, C. G., Pissis, P. *Thermochim. Acta* **2001**, *372*, 33.
31. Kremer, F.; Shoenhals, A., Eds. Broadband Dielectric Spectroscopy; Springer: New York, **2002**.
32. Brinker, C. W.; Scherer, G. W. In Sol-Gel Science—The Physics and Chemistry of Sol-Gel Processing; Academic Press: Boston; 1990, p 108–216.
33. Maciel, G. E. J. *J. Chem. Soc.* **1980**, *102*, 7606.
34. Mulder, D. *J. Non-Cryst. Sol.* **1987**, *93*, 169.
35. Gigant, K.; Posset, U.; Schottner, G.; Baia, L.; Kiefer, W.; Popp, J. *J. Sol-Gel Sci. Technol.* **2003**, *26*, 369.
36. Ceccorulli, G.; Pizzoli, M. *Polym. Bull.* **2001**, *47*, 283.
37. Bistac, S.; Schultz, J. *Prog. Org. Coat.* **1997**, *31*, 347.
38. Bistac, S.; Schultz, J. *Int. J. Adhes. Adhes.* **1997**, *17*, 197.
39. Wunderlich, B. *Prog. Polym. Sci.* **2003**, *28*, 383.
40. Fragiadakis, D.; Bokobza, L.; Pissis, P. *Polymer* **2011**, *52*, 3175.
41. He, F.; Wang, L.-M.; Richert, R. *Eur. Phys. J. Special Topics* **2007**, *141*, 3.
42. Hernandez, J. C. R.; Pradas, M. M.; Ribelles, J. L. G. *J. Non-Cryst. Sol.* **2008**, *354*, 1900.
43. Stathopoulos, A.; Klonos, P.; Kyritsis, A.; Pissis, P.; Christodoulides, C.; Hernandez, J. C. R.; Pradas, M. M.; Ribelles, J. L. G. *Eur. Polym. J.* **2010**, *46*, 101.
44. Stachurski, Z. H. *Polymer* **2002**, *43*, 7419.
45. Kalogeras, I. M. *J. Polym. Sci., Part B: Polym. Phys.* **2004**, *42*, 702.
46. Beiner, M. *Macromol. Rapid Commun.* **2001**, *22*, 869.
47. Alves, N. M.; Mano, N. M.; Ribelles, J. L. G.; Tejedor, J. A. G. *Polymer* **2004**, *45*, 1007.
48. Bergman, R.; Alvarez, F.; Alegria, A.; Colmenero, J. *J. Non--Cryst. Sol.* **1998**, 235–237, 580.
49. Rittigstein, P.; Torkelson, J. M. *J. Polym. Sci., Part B: Polym. Phys.* **2006**, *44*, 2935.
50. Schroetter, K.; Unger, R.; Reissig, F.; Garwe, F.; Kahle, S.; Beiner, M.; Donth, E. *Macromolecules* **1998**, *31*, 896.
51. Johari, G. P.; Goldstein, M. J. *J. Chem. Phys.* **1970**, *53*, 2372.
52. Ngai, K. L.; Gopalakrishnan, T. R.; Beiner, M. *Polymer* **2006**, *47*, 7222.
53. Schroetter, K.; Reissig, S.; Hempel, E.; Beiner, M. *J. Non--Cryst. Sol.* **2007**, *353*, 3976.
54. Bergman, R.; Alvarez, F.; Alegria, A.; Colmenero, J. *J. Chem. Phys.* **1998**, *109*, 7546.
55. Casalini, R.; Roland, C. M. *J. Non-Cryst. Sol.* **2011**, *357*, 282.
56. Boucher, V. M.; Cangialosi, D.; Alegria, A.; Colmenero, J.; Gonzalez-Irun, J.; Liz-Marzan, L. M. *Soft Matter* **2010**, *6*, 3306.
57. Boucher, V. M.; Cangialosi, D.; Alegria, A.; Colmenero, J. *Macromolecules* **2010**, *43*, 7594.
58. Kalogeras, I. M. *Acta Mater.* **2005**, *53*, 1621.
59. Raftopoulos, K. N.; Pandis, Ch.; Apekis, L.; Pissis, P.; Janowski, B.; Pielichowski, K.; Jaczewska, J. *Polymer* **2010**, *51*, 70.
60. Kripotou, S.; Pissis, P.; Bershtein, V. A.; Sysel, P.; Hobzova, R. *Polymer* **2003**, *44*, 2781.
61. Kyritsis, A.; Raftopoulos, K.; Rehim, M. A.; Shabaan, Sh. S.; Ghoneim, A.; Turky, G. *Polymer* **2009**, *50*, 4039.
62. Donth, E. The Glass Transition: Relaxation Dynamics in Liquids and Disordered Materials; Springer: Berlin, **2001**.
63. Berzosa, A. E.; Ribelles, J. L. G.; Kripotou, S.; Pissis, P. *Macromolecules* **2004**, *37*, 6472.
64. Garwe, F.; Schönhals, A.; Lockwenz, H.; Beiner, M.; Schrötter, K.; Donth, E. *Macromolecules* **1998**, *29*, 247.